GeoPatterns, Vol. V (2020), pp. 21-26, https://doi.org/10.5719/GeoP.5/3

InSAR digital terrain models for mining areas based on Sentinel-1 imagery. A case study in Căliman area

Mihaela GHEORGHE[1,2], Andrei-Ioan VODĂ MARC[1]

[1]University of Bucharest, Faculty of Geography
[2]GMV Innovating Solutions, Bucharest, Romania
mgheorghe@gmv.com

Abstract. Although not intended at first, SAR satellite technology has been used for digital terrain models (DTM) generation and displacement monitoring for the last 30 years starting with the launch of the first RADAR imaging satellite by the European Spatial Agency (ESA), ERS-1. Currently, there is a suite of satellites available for these applications, with ESA's Sentinel-1 being one of the most accessible and exploited by scientists due to its wide and free of costs availability. The C-band repeat-pass interferometer is considered unsuitable for DTM generation due to its acquisition geometry. In this study, a DTM based on Sentinel-1 imagery for the former sulphur quarry mine in Căliman Mountains is derived in order to demonstrate the potential of the dataset for time and cost effective monitoring of large areas.

Keywords: *InSAR; Digital terrain model, mining, Sentinel-1*

1. INTRODUCTION

The launch in 1978 of the first spaceborne imaging radar, SEASAT, by the National Aeronautics and Space Administration (NASA) showed for the first time the capability of Synthetic Aperture Radar (SAR) technology to capture reliable information about the Earth's surface physical properties, such as topography, morphology, dielectric properties, roughness and backscattering. The satellite SAR is an active system which operates within the microwave domain of the spectrum, being almost independent of meteorological conditions or illumination from external sources. Also, the side-looking geometry, the synthetic aperture and pulse compression technology increase achieved resolutions from tens of meters to a few meters.

Interferometric applications of SAR imaging data became popular with the launch of the ERS-1 satellite by the European Space Agency (ESA) in 1991, when various research groups investigated the method's potential with success (Bamler and Hartl, 1998, Klees and Massonnet, 1998, Ferretti et al., 2007, Smith., 2002, Hooper et al., 2004). Since then, the number of available SAR satellites increased rapidly, with the launch of Envisat, TerrasSAR, ALOS Palsar and Sentinel-1 satellites, today large datasets of SAR imagery offering a complete picture of the whole Earth's surface for the last 30 years. The applications based on SAR imagery are very diverse, such as digital terrain models generation, surface displacement monitoring, land classification, ice sheet monitoring, flood monitoring, etc (Cloude, 1997 Simons et al., 202, Stramondo et al., 2005, Rott, 2009, Pepe and Calo, 2017, Kussul, 2011). The most popular bands for lands surface applications are the X band ($\lambda \approx 3$ cm), C band ($\lambda \approx 5.6$ cm) and L band ($\lambda \approx 24$ cm).

Since the launch of Sentinel-1A satellite in April 2014, the first in ESA's Copernicus programme, the opportunities for accessing SAR imagery data increased substantially. Sentinel-1B satellite was launched in 2016, increasing the temporal resolution of the mission from 11 days to 5 days, which is unprecedented for SAR imagery. In terms of spatial resolution, Sentinel-1 can assure values of up to 5 m. Due to its wide free of cost availability, Sentinel-1 imagery was used in a large number of studies that focus mainly on displacement monitoring (Fiaschi et al., 2017, Huang et al., 2017, Raspini, 2018, Gheorghe et al., 2020). Due to its small baseline, the mission is not considered the best option for InSAR DEM generation. However, the current study aims to demonstrate that with the right selection of image pairs, a qualitative DEM can be obtained using Sentinel-1 C band imagery. In this purpose, the paper describes the general principles of InSAR and the methodology applied to derive a DEM of a mountainous area in Romania.

2. STUDY AREA

The study area is a former sulphur mining quarry of approximately 5 km^2 located in Căliman Mountains, which are found in the central-northern part of Romania. Pietrosul Căliman Peak is 2100 m high, which makes it the highest out of the mountainous group it belongs to: the Central Group of Eastern Carpathians. The mine used to be an industrial area of high importance in Romania, which was operational between 1969 and 1997. The quarry can be still found today on the northern slope of the Căliman massif, inside the mountain caldera Fig. 1). Since the cessation of activity, the study area continued to be affected by landslides, erosion and land failure, presenting also solid waste piled in the form of huge overburden dumps (Fig. 2). However, very few monitoring studies have been carried out in the area, especially due to the limited accessibility of the mining quarry, as well as the high costs of terrestrial surveying campaigns.

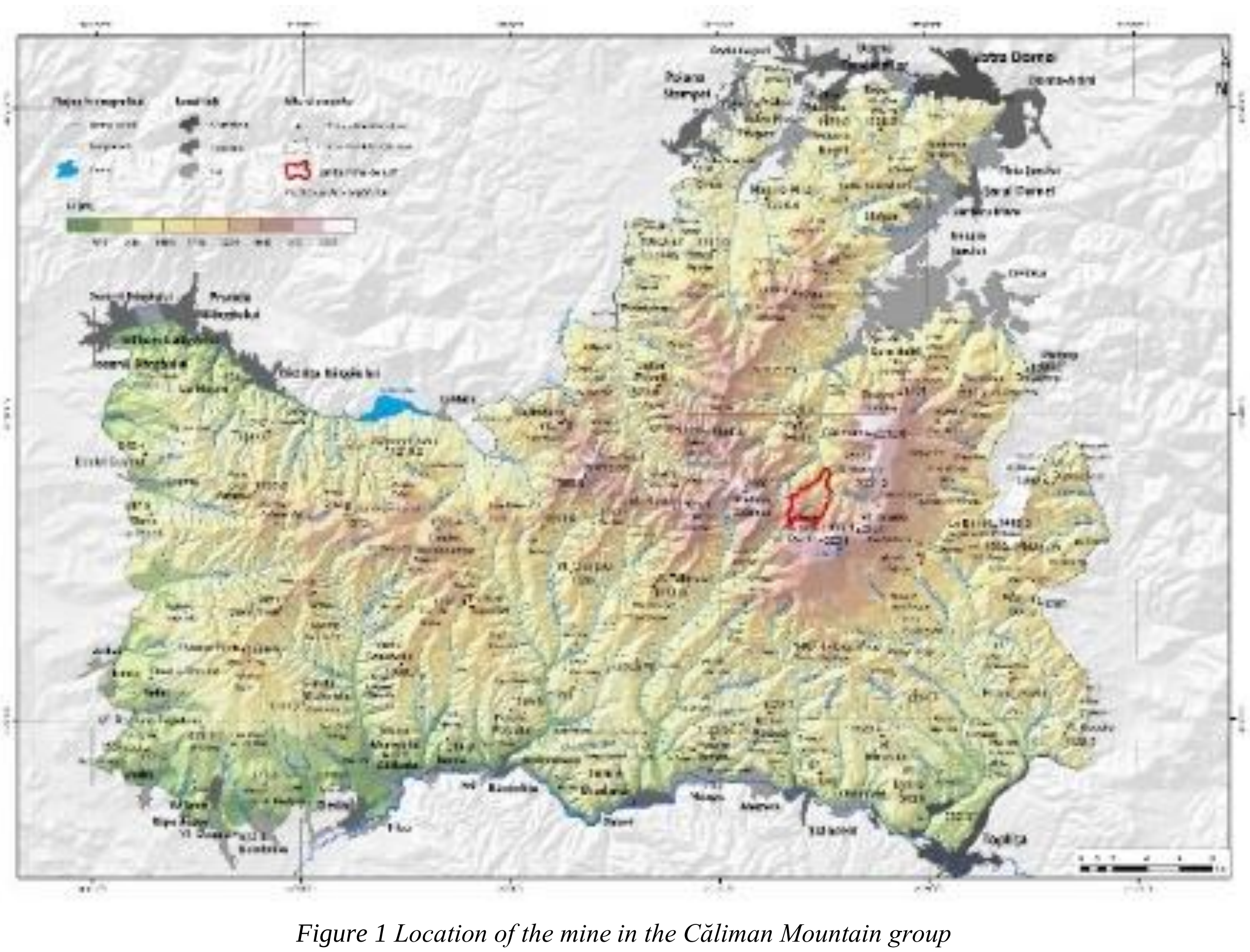

Figure 1 Location of the mine in the Căliman Mountain group

Figure 2 Satellite image of the actual state of the study area.
The overburden dumps due to solid waste are marked in red.

3. METHODOLOGY

Terrain reconstruction with SAR images is similar to conventional mapping using optical imagery. InSAR determines stereo parallaxes with an accuracy up to a fraction of a wavelength using the phase of the radar signal (Bamler and Hartl, 1998). The phase difference between two complex SAR images acquired for the same area from different points of view of the sensor is computed for each pixel. Sentinel-1 can be used as a repeat-pass interferometer based on images taken at different times, separated by days. Most of the single-pass spaceborne SAR were not considered optimal for InSAR applications because they were not initially designed with this application in mind (Bamler, 2003). Baselines (the spatial distance between two orbits) are especially important for InSAR applications (Fattahi and Amelung, 2013). Ideal baselines have to be long enough for the mapped area to be imagined from two different geometries but also not to exceed the optimal length for maintaining a good coherence between the images. A critical baseline ranges from 150 m up to 1000 m. Sentinel-1 orbits have short baselines, which are usually not suitable for DEM generation. For the current study, the selection of the image pair with a suitable baseline for DEM generation was the most challenging aspect.

The images selected for DEM geration are Single Looked Complex (SLC), acquired in Interferometric Wideswath (IW) mode products, with a perpendicular baseline of 124 meters. They were acquired 21 days apart by the Sentinel-1A satellite, on 8th of J\uly and 1st of August respectively on path 131, frame 149 (Fig. 3).

Figure 3 Extent of selected Sentinel-1 imagery

The processing chain for DTM extraction was implemented in the SNAP open source software provided by ESA. Sentinel-1 images are initially divided in multiple sub-swaths and bursts (Fig. 4).

The *TOPSAR-Split* operator, which is the first in InSAR processing chains, provides a convenient way of splitting each sub-swath and selected bursts into separate products.

The next step was *orbit correction*, which has the goal of removing orbital errors caused by inaccurate orbit state vectors provided in the metadata of a SAR product. The orbital correction necessitated precise orbit files which are available up to 14 days after the generation of the SLC product.

The *Back-geocoding* step refers to a DEM assisted coregistration. For this step, the SRTM 3Sec DEM was downloaded automatically and used as reference.

The *Enhanced Spectral Diversity* estimates a constant range offset for the whole sub-swath of the split image based on incoherent cross-correlation. The estimation is done individually for each burst, being averaged afterwards in order to derive a constant range offset available for the whole sub-swath.

The intermediary product was then exported for phase unwrapping in SNAPHU. Prior to the unwrapping step, a Goldstein filter was applied in order to reduce noise in the resulted interferogram. After filtering, the images were debursted, meaning that the bursts were concatenated and the sub-swaths merged to form a single-part image.

The *Interferogram* formation operator computed the complex interferogram with the subtraction of the flat-earth phase, since the orbits for the interferometric pair were known. The flat-earth phase is estimated from the orbital information and subtracted from the complex interferogram. The reference system of the surface is the same as the satellite orbits reference system, which is WGS84. The generated interferogram is imported back to SNAP for further processing

The next step is Phase to Elevation, which translates phase differences shown in the complex interferogram to corresponding elevation values of topography.

In the end, a *Terrain correction* is applied in order to compensate for the tilt of the satellite sensor in relation to topographical variations of a scene, which results in distorted distances in the SAR images.

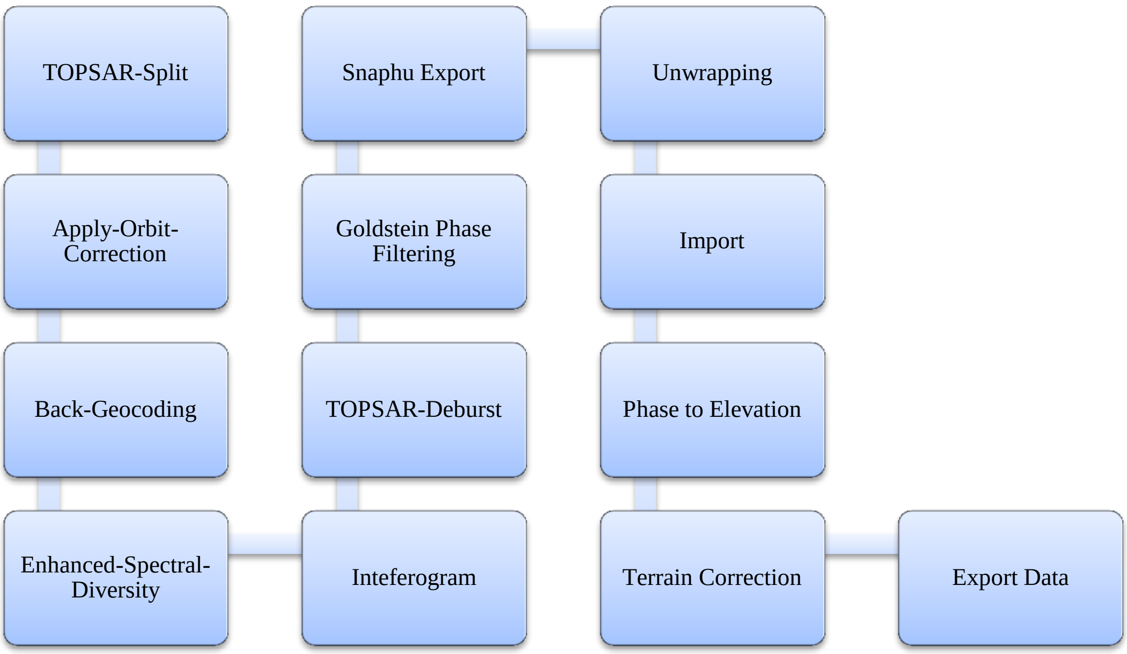

Figure 4 Processing chain for DEM generation in SNAP

4. RESULTS

The DTM extracted from satellite data has a resolution of 2.7x22m to 3.5x22m in range and azimuth respectively. The model was obtained in the same reference system as the satellite images, WGS 84 (EPSG 4326), Universal Transverse Mercator projection.

In order to assess the vertical accuracy of the DTM obtained from satellite imagery, it was projected in the Stereographic projection 1970, EPSG 3844 and compared to an older DTM derived from in-situ topography measurements conducted in the study area in 1980. The obtained DTM shows a 5 m vertical accuracy (Fig. 5).

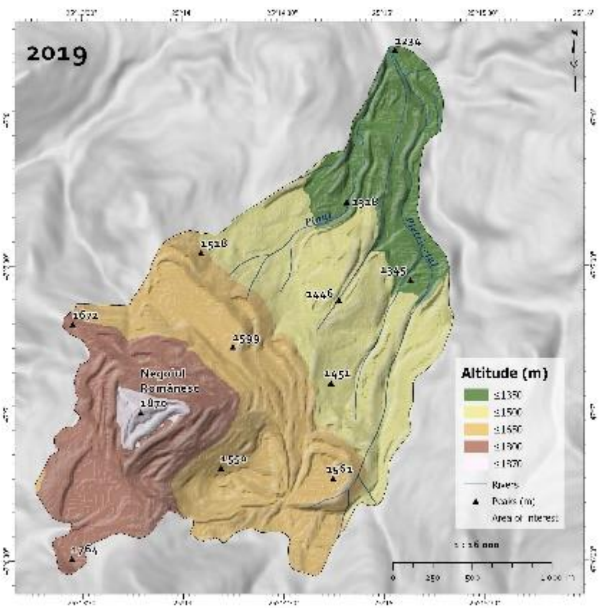

Figure 5 Digital Terrain Model of the Sulphur mining area extracted from Sentinel-1 imagery

5. CONCLUSION

Although a method more recent than optical stereo mapping InSAR has become more and more adopted for real life monitoring applications. DTMs obtained from SAR interferometers provide high resolution for local scales, while the SRTM mission was able to map the entire Earth within 11 days. The current paper explored the capability of Sentinel-1 imagery to provide an accurate DTM of a remote mining area found in the mountains. The obtained results show that a proper selection of acquisition geometry can lead to quality products. A great advantage of being able to use the Sentinel-1 imagery for any type of applications is given by the great volume of data available for all Earth.

The methodology employed in this study can be used for processing DTMs from a higher number of images for improving accuracy of the results that can change the approach for long-term monitoring.

REFERENCES

Klees, R., & Massonnet, D. (1998). Deformation measurements using SAR interferometry: potential and limitations. Geologie en Mijnbouw, 77(2), 161-176.

Ferretti, A., Monti-Guarnieri, A. V., Prati, C., Rocca, F., & Massonnet, D. (2007). INSAR Principles B. ESA publications.

Smith, L. C. (2002). Emerging applications of interferometric synthetic aperture radar (InSAR) in geomorphology and hydrology. Annals of the Association of American Geographers, 92(3), 385-398.

Bamler, R. & Hartl Ph. (1998). Synthetic aperture radar interferometry. Invers problems 14(4).

Hooper, A., Zebker, H., Segall, P., & Kampes, B. (2004). A new method for measuring deformation on volcanoes and other natural terrains using InSAR persistent scatterers. Geophysical research letters, 31(23).

Stramondo, S., Moro, M., Tolomei, C., Cinti, F. R., & Doumaz, F. (2005). InSAR surface displacement field and fault modelling for the 2003 Bam earthquake (southeastern Iran). Journal of Geodynamics, 40(2-3), 347-353.

Pepe, A., & Calò, F. (2017). A review of interferometric synthetic aperture RADAR (InSAR) multi-track approaches for the retrieval of Earth's surface displacements. Applied Sciences, 7(12), 1264.

Kussul, N., Shelestov, A., & Skakun, S. (2011). Flood monitoring from SAR data. In Use of Satellite and In-Situ Data to Improve Sustainability (pp. 19-29). Springer, Dordrecht.

Cloude, S. R., & Pottier, E. (1997). An entropy based classification scheme for land applications of polarimetric SAR. IEEE transactions on geoscience and remote sensing, 35(1), 68-78.

Simons, M., Fialko, Y., & Rivera, L. (2002). Coseismic deformation from the 1999 M w 7.1 Hector Mine, California, earthquake as inferred from InSAR and GPS observations. Bulletin of the Seismological Society of America, 92(4), 1390-1402.

Rott, H. (2009). Advances in interferometric synthetic aperture radar (InSAR) in earth system science. Progress in Physical Geography, 33(6), 769-791.

Raspini, F., Bianchini, S., Ciampalini, A., Del Soldato, M., Solari, L., Novali, F. & Casagli, N. (2018). Continuous, semi-automatic monitoring of ground deformation using Sentinel-1 satellites. Scientific reports, 8(1), 1-11.

Huang, Q., Crosetto, M., Monserrat, O., & Crippa, B. (2017). Displacement monitoring and modelling of a high-speed railway bridge using C-band Sentinel-1 data. ISPRS journal of photogrammetry and remote sensing, 128, 204-211.

Gheorghe, M., Armaș, I., Dumitru, P., Călin, A., Bădescu, O., & Necsoiu, M. (2020). Monitoring subway construction using Sentinel-1 data: a case study in Bucharest, Romania. International Journal of Remote Sensing, 41(7), 2644-2663.

Fiaschi, S., Tessitore, S., Bonì, R., Di Martire, D., Achilli, V., Borgstrom, S. & Calcaterra, D. (2017). From ERS-1/2 to Sentinel-1: Two decades of subsidence monitored through A-DInSAR techniques in the Ravenna area (Italy). GIScience & Remote Sensing, 54(3), 305-328.

Fattahi, H., & Amelung, F. (2013). DEM error correction in InSAR time series. IEEE Transactions on Geoscience and Remote Sensing, 51(7), 4249-4259.